(19) Europäisches Patentamt
European Patent Office
Office européen des brevets

(11) Publication number: **0 035 561**
B1

(12) # EUROPEAN PATENT SPECIFICATION

(45) Date of publication of patent specification: **02.09.87**

(51) Int. Cl.⁴: **H 01 L 21/263**, H 01 L 21/26

(21) Application number: **80901915.1**

(22) Date of filing: **08.09.80**

(86) International application number:
PCT/US80/01151

(87) International publication number:
WO 81/00789 19.03.81 Gazette 81/07

(54) **IMPROVED METHOD OF CRYSTALLIZING AMORPHOUS MATERIAL WITH A MOVING ENERGY BEAM.**

(30) Priority: **13.09.79 US 75010**
22.02.80 US 123745

(43) Date of publication of application:
16.09.81 Bulletin 81/37

(45) Publication of the grant of the patent:
02.09.87 Bulletin 87/36

(84) Designated Contracting States:
DE FR GB

(56) References cited:
WO-A-80/00510
US-A-3 585 088
US-A-4 045 674
US-A-4 059 461
US-A-4 087 695
US-A-4 147 563
US-A-4 155 779
US-A-4 187 126
US-A-4 198 246
US-A-4 203 781
US-A-4 229 232
US-A-4 234 358

(73) Proprietor: **MASSACHUSETTS INSTITUTE OF TECHNOLOGY**
77 Massachusetts Avenue
Cambridge, MA 02139 (US)

(72) Inventor: **FAN, John C. C.**
239 South Street
Chesnut Hill, MA 02167 (US)
Inventor: **ZEIGER, Herbert J.**
167 Pond Brook Road
Chesnut Hill, MA 02167 (US)

(74) Representative: **Holdcroft, James Gerald, Dr. et al**
Graham Watt & Co. Riverhead
Sevenoaks Kent TN13 2BN (GB)

(56) References cited:
APPLIED PHYSICS LETTERS, vol. 37, no. 3, 1st August 1980, pages 292-295, American Institute of Physics, New York, US; R.L. CHAPMAN et al.: "Crystallization-front velocity during scanned laser crystallization of amorphous Ge films"

EP 0 035 561 B1

Courier Press, Leamington Spa, England.

(56) References cited:
IBM TECHNICAL DISCLOSURE BULLETIN, vol. 19, no. 11, April 1977, pages 4438-4440, New York, US; P.S. HO et al.: "Multibeam method for growing large-grain semiconductor films"
APPLIED PHYSICS LETTERS, vol. 35, no. 1, 1st July 1979, pages 71-74, American Institute of Physics, New York, US; M.W. GEIS et al.: "Crystallographic orientation of silicon on an amorphous substrate using an artificial surface-relief grating and laser crystallization"
APPLIED PHYSICS LETTERS, vol. 27, no. 4, 15th August 1975, pages 224-226, American Institute of Physics, New York, US; J.C.C. FAN et el.: "Crystallization of amorphous silicon films by Nd:YAG laser hating"
Applied physics letters, 32(8), 15 April 1978, Celler et al., "Spatially controlled crystal regrowth of ion-implanted Si by laser irradiation", page 464-67
Solid state electronics, vol. 21, February 1978, "Campisano et al., "Laser reordering of implanted amorphous layers in GaAs", pages 485-488
Appl. physics letters, vol. 33 (2), 15 July 1978, Lau et al., "Epitaxial growth of deposited amorphous layer by laser annealing", page 130-131
IBM-Technical disclosure bulletin, vol. 22, no. 3, August 1979, (Armonk, N.Y.), Fang et al., "Stress-relieving annealing technique for SOS structures"
Soviet journal of quantum electronics, vol. 5, no. 10, 1976, (English, American Institute of Physics), Klimenko et al., "Use of argon laser radiation in restoration of single crystal state of ion-implantation amorphized Si surface", page 1289-1291
Applied physics letters, vol. 33(3), 1 August 1978, Bean et al, "Epitaxial laser crystallization of thin-film amorphous Silicon, page 227-230
IBM-Technical disclosure bulletin, vol. 19, no. 10, issued March 1977 (Armonk, N.Y.), Von Gutfeld, "Crystallization of Si for solar cell applications", page 3955-56
IEEE-Trans. electron devices, vol. ED-24, April 1977, Kirkpatrick et al., "Silicon solar cells by high speed low-temperature processing", page 429-432

Description

This invention relates to a method of converting solid amorphous materials, including amorphous semiconductor films, to a more crystalline state and to a use of this method in a method of fabricating a photovoltaic cell.

Background art

It has long been recognized that the efficiency of photovoltaic cells is lowered when the semiconductor material contains a high density of grain boundaries, which are present in polycrystalline semiconductors with small grains. Thus, the attainment of high cell efficiencies is dependent on the use of crystalline semiconductor materials which eliminate all or many of these grain boundaries, such as single crystal materials or polycrystalline materials which have large, preferentially aligned crystallites. On the other hand, the production of single crystal or large-grain polycrystalline semiconductor materials has heretofore been inordinately expensive, which has detracted from the economic competitiveness of energy produced from photovoltaic cells compared with energy from other sources, such as fossil fuel generated energy.

Because of this, much research has been directed to forming semiconductor films in an amorphous state and subsequently converting these amorphous materials to a crystalline state by rapid, inexpensive techniques. Many of these techniques have involved scanning amorphous semiconductors with a high power beam of energy, such as an electron beam or laser beam. Generally, such high power beams of energy cause localized heating and melting on the semiconductor material with subsequent cooling and crystallization as the beam advances.

An example of the use of a focused beam of electrons to recrystallize small areas on the surface layer of materials is described by Steigerwald in U.S. Patent No. 2,968,723. In a more specific application of an electron beam, Maserjian describes the production of single-crystal germanium films on sapphire substrates by heating the substrates to an elevated temperature and subsequently employing the electron beam to melt a small zone of polycrystalline germanium full thereon which forms single crystal germanium upon cooling. The substrate is heated to minimize the energy required by the electron beam which scans at a maximum frequency of 7 cm/sec. This process is stated by the author to be analogous to zone melting of semiconductor material. See Maserjian, J., "Single-Crystal Germanium Films By Micro-Zone Melting", *Solid State Electronics, 6,* Pergammon Press, 1963, pp. 477—84.

A two-step process and technique employing transient laser heating and melting to produce isolated regions of larger-grain polycrystalline silicon in films of fine-grain silicon on substrates such as fused silica has been described by Laff et al. See Laff, R. A. and Hutchins, G. L., *IEEE Transactions On Electron Devices,* Vol. ED-21, No. 11, Nov. 1974, p. 743. Because of certain disadvantages of such a laser-melting technique, others have employed radiant heating from a hot filament ribbon to give efficient thermal coupling to an amorphous silicon film in place of laser heating. See Von Gutfeld, "Crystallization of Silicon For Solar Cell Application", *IBM Technical Disclosure Bulletin, 19,* No. 10, March, 1977, pp. 3955—6.

Another method for improving the crystallinity of semiconductor materials by scanning them with a focused laser beam from a high-power laser suitably matched to the optical absorption properties of the semiconductor has previously been disclosed in our prior U.S. Patent No. 4,059,461, issued on November 22, 1977. An embodiment of the method patented in said US—A—4059461 involves the use of a focused beam from a Nd:YAG laser which is scanned across an amorphous silicon film at a rate sufficient to allow the film to heat to a temperature at which crystallization occurs. The Nd:YAG laser has been found to be particularly desirable with silicon films because of its relatively high overall power efficiency, its high power-output, and because it is well matched to the absorption characteristics of an amorphous silicon film since radiation is absorbed substantially uniformly across a thickness of about 10 µm. Large silicon crystallites are obtained after scanning, and it is even possible by the method according to US—A—4 059 461 to use a shaped laser spot, such as a slit, to provide a preferred crystalline orientation within the film. Of course, other semiconductors and other lasers can be used in this known method, as long as the laser wavelength and semiconductor are suitably matched and as long as the laser beam provides sufficient energy to improve the crystalline properties of the scanned film. It is particularly noteworthy that the method according to US—A—4 059 461 does not require that the semiconductor material be heated to a temperature above the melting point of the crystalline material to achieve crystallization. It is in fact preferred to carry this method out completely as a solid phase transformation.

Although our previously patented method has proven to be satisfactory for the crystallization of many semiconductor films, further experimentation did produce some unusual phenomena in certain cases. These included the formation of periodic structural features on semiconductor film surfaces, pulsations of film temperature during scanning, and runaway crystallization of an entire film following first contact with a laser image. Such phenomena were initially not well understood.

IBM Technical Disclosure Bulletin, Vol. 19. No. 11, April 1977 at pages 4438—4440 contains a paper entitled "Multibeam Method For Growing Large-Grain Semiconductor Films". This paper discloses a method of converting solid amorphous material, without melting it, to a more crystalline state, wherein the material is maintained at a first temperature and is irradiated with an energy beam which is scanned over the material to raise it to a second temperature whereat crystal growth occurs within the influence of the beam.

According to the present invention, there is provided a method of converting solid amorphous material, without melting it, to a more crystalline state, wherein the material is maintained at a first temperature and is irradiated with an energy beam which is scanned over the material to raise it to a second temperature whereat crystal growth occurs within the influence of the beam, characterised by keeping the material at a background temperature T_b below a runaway temperature T_r at which self-sustaining crystallization occurs and by the energy beam having an intensity sufficient to raise the material locally to a critical temperature T_c at which transformation to a crystalline state occurs instantaneously, whereby a crystallization front travels in advance of the beam, the rate at which the beam is scanned being such that before the temperature at the crystallization front quenches below T_c, the material adjacent the advancing crystallization front is heated by the beam sufficiently to prevent the temperature thereat quenching below T_c, the prevention of quenching avoiding the formation of a periodic crystallization structure.

The invention described herein arises out of our further investigation into the unusual phenomena which sometimes occur with the laser crystallization techniques disclosed in U.S. 4,059,461. These further investigations include the generation of a theoretical model which can be used to predict the unusual phenomena previously observed with some film crystallizations. Because of such investigations, we have now discovered how to provide continuous, controlled motion of the crystallization front in an amorphous material by controlling parameters such as the rate at which the laser beam or other beam of energy is moved across an amorphous material and the temperature of the substrate.

In practising our invention, amorphous material is converted to a more crystalline state by moving an energy beam across the material under conditions which provide continuous, controlled motion of the crystallization front. One aspect of controlling the crystallization front relates to the scanning rate of the energy beam, which in the case of this invention is typically higher for most materials than scan rates previously employed with the same materials. The crystallization efficiency of these increased scan rates is surprising particularly in view of those prior art teachings in which the beam energy was employed to heat local areas of an amorphous or polycrystalline material to a molten state. Unlike crystallizations achieved by heating the material to a temperature above the melting point of the crystalline material, the crystallizations achieved by this invention are done in the solid phase. Such solid phase transformations allow lower temperatures to be employed, are extremely rapid, and result in crystallized materials having exceptionally smooth surfaces.

Another aspect of controlling the crystallization front, described hereinafter, relates to modulation of the energy beam, and in particular, spatial and/or temporal modulation of the beam intensity. In general, any modulation is sufficient that provides a crystallization front which advances fast enough to avoid quenching and periodic structure while also avoiding crystallization front runaway.

Thus, this invention offers many advantages over prior techniques for crystallizing amorphous materials, and in general, permits the rapid, uniform, solid-phase conversion of a wide variety of amorphous material to a more crystalline state.

An embodiment of the invention will now be explained in more detail in the following non-limitative description, taken in conjunction with the accompanying drawings, in which:

Fig. 1 is a schematic view of an apparatus suitable for scanning amorphous material with a laser beam as described herein;

Fig. 2 is an optical transmission micrograph of a laser-crystallized germanium film having periodic structural features;

Fig. 3 is an exploded view of a small area of the micrograph of Fig. 2;

Fig. 4 is a bright-field transmission electron micrograph of a laser-crystallized germanium film;

Figs. 5 and 6 are transmission electron diffraction patterns for fine-grained and large-grained regions of a laser-crystallized germanium film;

Fig. 7 is a schematic diagram illustrating the crystallization of an amorphous semiconductor film by a scanned slit laser image;

Fig. 8 is a plot of normalized position of amorphous-crystalline phase boundary with respect to a laser image as a function of normalized time obtained from the theoretical model for various given parameters;

Fig. 9 is a plot of theoretical and experimental data for spatial periodicity ratio vs. temperature ratio for laser-crystallization of a germanium film;

Fig. 10 is a plot of theoretical and experimental data for the spatial period structural features of laser-crystallized germanium films as a function of background temperature;

Fig. 11 is a block diagram which illustrates one method for fabricating a photovoltaic cell employing laser beam scanning of a semiconductor film as described herein;

Fig. 12 is a cross-sectional view of a photovoltaic cell which could be prepared by the method illustrated in Fig. 11;

Fig. 13 is a block diagram which illustrates an alternative method for fabricating a photovoltaic cell employing laser beam scanning of the semiconductor film as described herein;

Fig. 14 is a cross-sectional view of a photovoltaic cell which could be prepared by the method illustrated in Fig. 13;

Fig. 15 is a block diagram which illustrates still another alternative method for fabricating a photovoltaic cell employing laser beam scanning of a semiconductor film as described herein;

Fig. 16 is a cross-sectional view of a photovoltaic cell prepared by the method illustrated in Fig. 15;

Fig. 17 is a schematic diagram illustrating crystallization according to this invention with a spatially and temporally modulated energy beam;

Fig. 18 is a schematic diagram of an apparatus suitable for crystallizing amorphous materials according to this invention by employing an electron beam or an ion beam; and,

Fig. 19 is a schematic diagram of an apparatus for crystallizing amorphous materials according to this invention employing a train of electrical pulses simulating a moving energy beam.

Best mode of carrying out the invention

The invention will now be further described with particular reference to the Figures.

An apparatus suitable for scanning semiconductor films with a focused laser beam is illustrated in Fig. 1. Laser 10, which is a high power, high efficiency laser, such as a Nd:YAG laser, emits laser beam 12 which is focused to a spot having the shape and size desired by focusing lens 14. A preferred shape is one which has a large aspect ratio, such as an elongated slit, because such shapes can be used to align semiconductor crystallites as well as to enlarge them. This is apparently because the slit produces thermal gradients in the semiconductor film transverse to its long axis. Because of these temperature gradients, crystallization of the film results in a preferred alignment and growing, aligned domains then tend to coalesce as the scanning continues producing larger, more aligned grains.

The exact size and shape of the focused laser spot will depend upon factors such as laser power, scanning rate, area to be scanned, crystalline properties desired, etc. Various shapes are obtainable by employing beam expanders, cylindrical lenses, mirrors, or other optical or mechanical elements known to those skilled in the art. For reasons of practicality, it is preferred to use a spot size having an area of at least about 10^{-4} cm^2. It is also particularly preferred, as mentioned above, to employ a laser image having a large aspect ratio. For example, if the beam is rectangular in shape, it is preferred to have the aspect ratio (1/w) greater than 10. Large aspect ratios provide uniform temperature gradients which, in turn, promote aligned crystallites.

Beam splitter 16 is used to divide focused beam 12 so that a first portion is reflected to power detector 18 and a second portion is transmitted to electro-optical scanner 20. Power detector 18 serves to measure the exact beam power so that any desired changes in laser power, scanning rate, etc., can be made. Electro-optical scanner 20 is one convenient means for scanning focused beam 12. After passing scanner 20, focused beam 12 enters sample chamber 22 through transparent window 24 and strikes the surface of semiconductor 26.

Scanning of semiconductor 26 can be achieved by mounting sample chamber 22 upon three translational stages, 28, 30 and 32. Translational stages 28, 30 and 32 provide the capability to move chamber 22, and thus semiconductor 26, in the x, y and z directions, respectively. Each stage can be independently driven by connecting rotatable arms 34, 36 and 38 to electric motors (not shown). Each stage can be driven separately, or any combination can be driven simultaneously. Also, the rate at which each stage can be driven is variable. Thus, a great variety of scan patterns and rates is achievable.

Of course, electro-optic or acousto-optical beam deflectors or other means to raster the laser beam can also be used, and these are known to those skilled in the art. In fact, scanning can be achieved by moving either the sample or the beam, or both.

The scan rate is set, of course, by the dwell time required. As a general rule, however, the scan rates used with this invention are higher than those used with prior methods.

Radiant heating lamp 40 can be used to help heat the semiconductor 26. Induction heaters, resistance heaters, or other means to heat semiconductor 26 could, of course, also be employed.

The apparatus illustrated in Fig. 1 is typical of that employed in our previous patent, U.S. 4,059,461. The teachings of our prior patent are hereby incorporated by reference, particularly in regard to other suitable apparatus for carrying out a laser-crystallization process and for matching the characteristics of the laser to the amorphous material to be scanned as well as the determination of other appropriate parameters for the method.

To investigate some of the unusual phenomena sometimes observed in laser crystallizations, a crystallization system utilizing a cw Nd:YAG laser beam focused to a slit image with power density that is uniform to ±3% over a central area about 50 μm by 1.5 mm was employed. The samples were placed in an Ar/H_2 atmosphere on a resistively-heated platform that permitted them to be scanned at various rates obtained by using synchronous motors, under the laser beam in the focal plane and normal to the long axis of the slit image. This apparatus is described in more detail in the following references, the teachings of which are hereby incorporated by reference: J. C. C. Fan, H. J. Zeiger, and P. M. Zavracky, Proc. Nat. Workshop on Low Cost Polycrystalline Silicon Solar Cells, Dallas, 1976, edited by T. L. Chu and S. S. Chu (Southern Methodist University, Dallas, 1976), p. 89; and J. C. C. Fan, J. P. Donnelly, C. O. Bozler, and R. L. Chapman, Proc. 7th Int. Symp. on GaAs and Related Compounds, St. Louis, 1978, Institute of Phys. Conf. Ser. No. *45*, Chapter 6, p. 472 (1979). Amorphous germanium (a-Ge) films were deposited by either electron-beam evaporation, rf sputtering, or ion-beam sputtering on molybdenum, graphite, or fused-silica substrates.

In initial experiments on a-Ge films 2—4 micrometers thick on molybdenum and graphite substrates, the platform was heated to maintain the temperature of the film before laser irradiation (T_b) at 400—500°C.

Once crystallization was initiated by momentary irradiation at a single point, the transformation was found to be self-sustaining, with the crystallization front rapidly propagating radially outward from the irradiated spot. Films as large as 2.5 cm×2.5 cm were entirely crystallized in this manner. At lower values of T_b self-sustaining crystallization did not occur, but laser scanning yielded areas of elongated, well-aligned grains. The surface of the scanned films remained smooth, regardless of T_b. The maximum temperature reached by the film during scanning, estimated from its color, was about 700°C, far below the melting point of crystalline Ge, which is about 937°C. Because of this, the transformations from amorphous to crystalline described herein are referred to as "solid phase transformations". This means that the maximum temperature reached by the material as a result of the energy beam is below the melting point of the crystalline phase of the material.

A series of laser scanning experiments on films about 0.3 μm thick deposited by electron-beam evaporation on 1-mm thick fused silica substrates was then performed. The power density of the central area of the laser image was kept at about 5 kW/cm², and the scan rate at 0.5 cm/sec. The background temperature T_b, which was found to be critical in crystallization behavior, was varied from room temperature to 500°C. For T_b equal to room temperature, after laser scanning, the films exhibited periodic structural features. Within each film the spatial period initially increased, but after several periods, it reached a steady-state value of about 50 μm. Fig. 2 shows an optical transmission micrograph of one such film, obtained with visible radiation from a xenon lamp. The dark areas in the micrograph are regions of untransformed a-Ge, which for the film thickness used was almost opaque to visible and near-infrared radiation, while the bright areas are regions of crystalline Ge, which had significant transmission in the red and near-infrared. Similar contrast was also obtained using infrared microscopy. Each periodic feature consisted of four different regions, as shown in Fig. 3. These were a narrow amorphous region, followed by another region containing a mixture of amorphous material and fine grains, and then a broad region of fine crystallites, and finally another broad region of much larger, elongated crystallites having dimensions of about 1—2×20 micrometers, generally aligned parallel to each other but at an angle of about 55° to the laser scan direction. In the films examined in detail, it was noted that the large crystallites within each periodic feature formed a roughly chevron-like pattern, with the two halves of the pattern symmetrical about an axis parallel to the scan direction and located near the center of the laser slit image. Thus, the angles between the long axes of the crystallites and the scan direction were similar in magnitude but of opposite sense for the two halves of the pattern. In the micrograph of Fig. 2, the symmetry axis lies close to or just below the bottom of the micrograph, so that only half the chevron pattern can be seen.

The optical microscopy results were confirmed by transmission electron microscopy (TEM) using 125 keV electrons. The TEM samples were removed from their substrates using hydrofluoric acid to partially dissolve the fused silica. Fig. 4 is a TEM bright-field micrograph of a portion of a film that was laser-scanned with T_b equal to room temperature. The micrograph illustrates the same sequence of regions found by optical microscopy and shown in Fig. 2: amorphous (the dark area), amorphous-plus-crystalline, fine-grain and large-grain. The fine-grain region yields a transmission electron diffraction pattern like the one shown in Fig. 5, with the rings typical of polycrystalline material. Within this region, the grain size gradually increases until it reaches about 0.3 μm, the thickness of the film, then increases abruptly to give the large, well-aligned crystallites of the final region, which are clearly visible as ribbon-like structures in the lower left corner of the micrograph of Fig. 4. This is the end portion of the preceding periodic feature. It has been demonstrated by bright-field and dark-field TEM that each of these structures is a single grain, and that they yield characteristic single-crystal transmission electron diffraction patterns. Fig. 6 is an example of such a diffraction pattern. This pattern indicates that the crystallites are oriented with the normal to the plane of the substrate in a <110> direction, their long axis in a <001> direction, and a <112> direction parallel to the long axis of the laser slit image. These orientations are clearly characteristic of the solid-phase growth process described herein, since they are the same for the large crystallites throughout the film, even though these crystallites in successive periodic features are separated by regions of amorphous and randomly oriented, fine-grain material. The above experiments were repeated using values of background temperature T_b that were above room temperature but not high enough to result in self-sustaining crystallization, and the resulting scanned films exhibited periodic structural features similar to those described above.

In an effort to explain the periodic structural features formed as a result of laser scanning, the dependence of the spatial period on T_b, and the occurrence of self-sustaining crystallization at values of T_b greater than the runaway temperature T_r, a theoretical model for the dynamics of the scanned laser crystallization of an amorphous film was developed. Although the following discussion is set forth in terms of a specific system, i.e., laser scanning an amorphous semiconductor film, it should be recognized that the mathematical model produced applies very generally to other systems, and specifically to moving energy beams other than lasers and amorphous materials other than semiconductor films.

Fig. 7 is a schematic diagram illustrating the geometry considered. The film is deposited on a thick substrate that is heated to T_b, and the laser image is scanned from left to right at velocity v. The approximation was made that the amorphous-crystalline (a-c) transformation occurs instantaneously when the film reaches a critical temperature T_c. The basis for this approximation is that the rate of transformation increases exponentially with temperature. See Blum, N. A. and Feldman, C., *J. Non-Cryst. Solids, 22,* 29 (1976). This means that over a narrow temperature interval the ratio of the time required for transformation

to the time required for laser scan changes from $\gg 1$ to $\ll 1$. The a-c boundary therefore coincides with a T_c isotherm, and the motion of the boundary can be found by calculating the motion of the isotherm.

Crystallization of the amorphous film, accompanied by liberation of latent heat, begins when the film temperature reaches T_c along a line at the left edge of the film that is parallel to the long axis of the laser image. Because the film temperature ahead of the image is then increased by conduction of the latent heat as well as by laser heating, the T_c isotherm, and therefore the a-c boundary, move to the right at a velocity v_{ac} that is initially much higher than v. As the boundary moves away from the laser image, the contribution of laser heating to the temperature at the boundary decreases rapidly. The continuing liberation of latent heat tends to maintain the forward motion of the boundary, but if T_b is less than T_r, heat conduction within the film eventually reduces the boundary temperature below T_c, and the boundary abruptly stops moving. At this time, there is a region of crystallized material between the laser image and the left edge of the untransformed film. The boundary then remains at rest until its temperature is increased to T_c by the approaching laser image, and the whole process is repeated. Thus, although the laser image is scanned at a constant velocity, the a-c boundary moves in a series of rapid jumps between rest positions. According to the model, the periodic structural features of the laser-scanned film are due to this periodic motion of the boundary, and the spatial period of these features is the distance between successive rest positions. With increasing T_b, this distance increases, since less heat is required to increase the film temperature to T_c, so that the a-c boundary moves farther beyond the laser image before it comes to rest. If T_b exceeds T_r, the continuing release of latent heat is sufficient to maintain the propagation of the T_c isotherm indefinitely, resulting in self-sustaining crystallization. Such self-sustaining crystallization does not result in large, aligned crystallites.

The actual derivation of the theoretical model will now be given.

The semiconductor film, which is deposited on a thick substrate of poor thermal conductivity, is of infinite extent in the y and z directions and so thin that its temperature is constant in the x direction. The laser slit image is of infinite length in the z direction and moves at a velocity v from left to right in the y direction. At $t=0$, the phase boundary is located at y_o, with the crystalline phase to the left ($y<y_o$) and the untransformed amorphous phase to the right ($y>y_o$). The laser image carries with it a steady temperature profile T_1 $(y-vt)$. At $t=0$, the temperature at the phase boundary reaches T_c and the boundary begins to move toward the right, with heat being liberated at a rate per boundary unit cross-sectional area of $fL\rho\dot{Y}(t)$, where L is the latent heat of a—c transformation of the semiconductor, ρ is the semiconductor density, Y(t) is the position of the boundary at time t, and f is a factor less than 1 that accounts in an approximate way for the loss of latent heat to the substrate. Then the temperature T(y, t) at any point y along the film at time t is given by the one-dimensional integral relation

$$T(y,\ t)=T_1(y-vt)+\frac{fL}{C}\frac{1}{2(\pi\kappa)^{1/2}}\int_o^t\frac{\dot{Y}(t')}{(t-t')^{1/2}}\exp\left\{\frac{-[y-Y(t')]^2}{4\kappa(t-t')}\right\}dt' \qquad (1)$$

where C is the specific heat of the film, $\kappa=K/C\rho$ defines its thermal diffusivity, and K is its thermal conductivity. An integral equation for Y(t) can be obtained by using the condition that the temperature at the phase boundary is T_c or

$$T[Y(t),\ t]=T_c \qquad (2)$$

For purposes of calculation, it is convenient to rewrite Eq. (2) in the frame of reference moving with the laser image. For this purpose, the position variable $u(t)=y(t)-vt$ is introduced, where u(t) is measured from the center of the laser image as origin. The temperature T_1 is modeled in the form $T_1(u)=T_b+\Delta T_i \exp[-(u/a^2)]$, where T_b is a uniform time-independent background temperature and the temperature contribution due to the laser is described by a Gaussian of width a and magnitude ΔT_i. Finally, introducing normalized quantities, the integral equation for the motion of the phase boundary can be written as

$$1=\sigma\exp\{-[S(T)]^2\}$$

$$+\eta\int_o^{\cdot}\{[\dot{S}(T')+V]/(T-T')^{1/2}\}\exp\{-[S(T)-S(T')+V(T-T')]^2/(T-T')\}dT' \qquad (3)$$

where $\sigma=\Delta T_i/(T_c-T_b)$ (4a)

$$\eta=fL/C\pi^{1/2}(T_c-T_b) \qquad (4b)$$

$T\equiv 4kT/a^2$, $V\equiv av/4\kappa$, $S\equiv U/a$, $\dot{S}(T')\equiv[dS(T')/dT']=(1/a)[dU(T')/dT']dt'/dt'$, and

U is the position of the phase boundary measured from the center of the laser image.

Equation (3) is not in itself sufficient to give physically acceptable solutions for the motion of the phase boundary, since it allows negative values of $[\dot{S}(T')+V]$, which imply a motion of the phase boundary back

toward the laser image, with the reconversion of crystalline material to the amorphous state, accompanied by the reabsorption of latent heat. To constrain Eq. (3) to physically acceptable solutions it is required that, when the numerical solution of Eq. (3) yields $[\dot{S}(T')+V]\leq 0$, this quantity is to be set equal to zero, with the phase boundary remaining stationary.

Equation (3) has been solved numerically to obtain S as a function of T for representative values of α, η, and V, with the boundary conditions that $S(T)=0$ at $T=0$ and that $S(0)$ is given by $1=\alpha \exp\{-[S(0)^2]\}$. The inset of Fig. 8 calculated for $\alpha=3.6$, $\eta=0.6$, and $V=0.3$, depicts the approach to the steady state oscillatory type of solution characteristic of Eq. (3). Fig. 8 shows plots of S vs T for $V=0.3$ and three increasing values of η, with α increasing in proportion to η (which corresponds, from Eqs. (4a) and (4b), to increasing T_b toward T_c while holding ΔT_l fixed). For each value of η, S initially increases rapidly because the latent heat liberated by the phase transformation raises the temperature ahead of the boundary, accelerating its forward motion. As the boundary moves away from the laser image, the contribution of the laser to the temperature ahead of the boundary decreases rapidly. For $\eta=0.3$ the boundary motion soon decelerates, and the boundary comes to rest, remaining fixed for a time interval during which its temperature initially drops rapidly below T_c and S decreases with velocity $\dot{S}=-V$. With the approach of the laser image, the boundary temperature gradually increases to T_c, the boundary once more moves forward, and S again increases. This cycle is repeated indefinitely, resulting in the oscillations in S seen for $\eta=0.3$ in Fig. 8.

When η is increased by increasing T_b, less latent heat is required to heat the film to T_c ahead of the laser image, and the phase boundary moves farther beyond the laser before it decelerates and comes to rest. This trend is illustrated by the calculated curve for $\eta=0.6$ in Fig. 8, and leads to periodic motion with a longer period. When η becomes large enough, the heat liberated during crystallization is sufficient to sustain the transformation, causing the boundary to "run away" from the laser image. This situation, which is illustrated by the curve for $\eta=0.8$ in Fig. 8, accounts for the observation that the entire film is crystallized following momentary contact with the laser image.

For the three curves shown in Fig. 8, the average value of $\dot{S}(T)$ during each of the times when the phase boundary is moving ahead of the laser image is seen to be approximately the same and essentially independent of η.

In addition to explaining runaway crystallization, the proposed model can also explain other qualitative observations on laser crystallization. For example, different regions of such films can be expected to differ in microstructure depending on their rates of transformation and therefore on their thermal history. This suggests that the periodic structural features observed on laser-crystallized films, such as that seen in Fig. 2, can be attributed to oscillations in S like those implied by the curves for $\eta=0.3$ and 0.6 in Fig. 8. Furthermore, for sufficiently high values of η these oscillations produce large fluctuations in the rate of heat liberation and therefore in temperature. This can explain the periodic fluctuations in color temperature observed during some laser crystallization experiments.

In order to carry out a semi-quantitative test of the model, the spatial period of the structural features of laser-crystallized Ge films was determined as a function of T_b. Experiments were performed on amorphous films 0.3 μm thick, deposited on fused silica substrates and scanned at v=0.5 cm/sec with the slit image of a cw Nd:YAG laser. Initially, a film at room temperature was irradiated at a laser power level just high enough to produce crystallization, which yielded structure in the transformed film with a spatial period of ~50 μm. In the following experiments each film was heated to a successively higher value of T_b, the laser scanned at the same power level, and the spacing measured after crystallization. This procedure was continued until T_b approached the value resulting in runaway.

To use the model to calculate the spatial period in the film, it was assumed that this period was equal to the distance ΔY traversed by the a–c phase boundary during each of its successive jumps, from the point where crystallization is initiated by the approaching laser to the point where the boundary comes to rest ahead of the laser. This distance is just equal to $(V\Delta T)$, where V is the normalized laser scanning velocity and ΔT is the normalized time interval between the beginnings of two successive jumps, i.e., the period of the oscillations in S illustrated by the curves for $\eta=0.3$ and 0.6 in Fig. 8.

To obtain a relationship between ΔY and T_b, Eq. (3) was first used to calculate $V\Delta\tau$ as a function of η for representative values of α and V: The calculated curve for $\alpha=6\eta$ (corresponding to fixed ΔT_l) and $V=0.3$ is shown in the inset of Fig. 9. With increasing η, $\Delta\tau$ and therefore $V\Delta\tau$ increase rapidly, leading to boundary runaway by $\eta=0.65$. For a given value of η, $V\Delta\tau$ was found to be quite insensitive to either α or V, showing that the boundary jump distance is determined primarily by the properties of the film and by T_b, and does not depend strongly on either the power or velocity of the laser.

In order to compare theory with experiment, the curve of $V\Delta\tau$ vs η shown in the inset of Fig. 9 was used to obtain curves relating the ratios $\Delta Y/\Delta Y_o$ and T_b/T_c, where ΔY_o is the spatial period in the film (i.e., the boundary jump distance) for T_b of room temperature. To calculate these curves, Eq. (4b) was rewritten in the lumped-parameter form $\eta=\eta_o/(1-T_b/T_c)$, where $\eta_o \equiv fL/\pi^{1/2}CT_c$. If T_b and T_c are expressed in °C, room temperature is much less than T_c, so that $\eta_o \approx \eta$ at room temperature, and ΔY_o corresponds to η_o. Curves of $\Delta Y/\Delta Y_o$ vs $T_b/T_c=1-\eta_o/\eta$ were calculated by adopting pairs of numerical values of η_o and T_c, then compared with the experimental-points (for each point, the adopted value of T_c was used to determine T_b/T_c). A reasonable overall fit has been obtained, as shown in Fig. 9, for $\eta_o=0.14$ and $T_c=685$°C. The abrupt increase in $\Delta Y/\Delta Y_o$ when T_b/T_c exceeds about 0.7 is associated with the approach of T_b to the value T_r above which laser irradiation results in boundary runaway. From the calculations, T_r is about 0.775 T_c=530°C.

From the definition of η_o, $fL=\pi^{1/2}CT_c\eta_o$. Taking C=0.08 cal/g°C for amorphous Ge and the values of T_c and η_o used for Fig. 9, fL=13.6 cal/g. In calorimetric measurements made during the rapid heating of amorphous Ge films, Chen and Turnbull observed a sharp transition at ~500°C and measured L=37.1 cal/g. See H. S. Chen and D. Turnbull, *J. Appl. Phys., 40,* 4214 (1969). Using the model result for fL gave a value of only about 1/3 for f.

The Gaussian width of the laser temperature profile can be determined from the relationship $a=\Delta Y/V\Delta\tau$. From the measured ΔY_o=50 μm at room temperature and $V\Delta\tau\leq 0.25$ corresponding to η_o in the inset of Fig. 9, a ~200 μm. The phase boundary velocity V_{ac} can then be determined from the normalized boundary velocity V_{ac}~1.9 by using the relation $v_{ac}=4\kappa V_{ac}/a$. For $\kappa=K/\rho C$, a value of 0.09 cm^2/sec is estimated by taking K=0.035 cal/cm sec °C, $\rho\approx 5$ g/cm^3, and C=0.08 cal/g°C. The value obtained for V_{ac} is then ~35 cm/sec, much higher than the laser scan velocity v=0.5 cm/sec.

The value obtained for the front velocity, V_{ac}, is dependent upon the time interval $\delta\tau$ for numerical integration, and represents a lower limit, since smaller values of δt lead to higher values of V_{ac}. The values obtained from the calculation for the spatial period of the oscillations are, however, independent of $\delta\tau$. Results of preliminary measurements of V_{ac} for a 0.3 μm film of amorphous germanium indicate that the value for V_{ac} is between 150 and 400 cm/sec. The exact V_{ac} value will depend upon such variables as film thickness, the particular semiconductor, and the substrate material and temperature. In all cases, the front velocity, V_{ac}, is much higher than the scan velocity.

Fig. 10 presents the experimental and theoretical data obtained in a slightly different manner. The points shown are the experimental data whereas the computer solution of Eq. 3 is plotted as a continuous curve. From these data, it can be appreciated that larger, aligned crystallites are produced by longer spatial periods.

From the above, it can be seen that the scan rate of the laser beam or other energy beam, can be used itself or in conjunction with the background temperature to achieve a quasi-continuous, controlled motion of the crystallization front. The scan rate can be much more rapid than has traditionally been employed which is possible because of the solid phase nature of the amorphous-crystalline transformation. Of course, the scan rate of the laser beam or other energy beam need not be continuous, but may itself be pulsed in a manner which applies a pulse of energy to the crystallization front prior to the time that the front would quench to a temperature which would result in periodic structure.

Fig. 11 illustrates diagrammatically the fabrication of a photovoltaic cell employing the laser scanning procedure described herein, and Fig. 12 illustrates a cell produced thereby. The first step in this fabrication is the formation of a conductive layer 52 on a substrate 50. This could be achieved, for example, by vacuum depositing a metal layer such as copper, silver, tin, gold or other metal onto substrate 50. Substrate 50 need not be transparent, but certainly could be. Also, substrate 50 itself could be conducting, which satisfies the first step in this fabrication.

Then, a film of amorphous semiconductor 54 is deposited onto conducting layer 52 or directly onto substrate 50 if it is conducting. An example is a deposition of a thin film of silicon during the final step in the preparation of pure silicon by a method such as the chlorosilane process. Thus, the cost of the amorphous silicon film could be covered in the silicon purification step. Any suitable semiconductor deposition process which provided the purity required could be used, of course, since the usual crystalline perfection requirements are not present because the semiconductor film will undergo laser beam or other energy beam scanning.

Amorphous semiconductor film 54 is then scanned with a focused laser beam from a high power laser to improve its crystalline properties. This might be achieved, for example, in the case of an amorphous silicon film by the mechanical linear sweep of the silicon sheet under a slit image from a Nd:YAG laser and/or with the slit image scanned laterally back and forth by an acousto-optic or electro-optic scanner.

Finally, a transparent rectifying contact 56 is formed with a laser-scanned semiconductor film 54. This could be done, for example, by depositing a transparent, highly conducting tin-doped indium oxide film over a thin transparent metallic layer to form a Schottky barrier. Suitable tin-doped indium oxide films are described in Fan, J.C.C., and Bachner, F. J., *J. Electro Chem. Soc., 122,* 1719 (1975), the teachings of which are hereby incorporated by reference. Alternatively, a rectifying contact would be formed by laser scanning in a doping atmosphere to form a p–n junction at the surface of the laser-scanned film.

As illustrated in Fig. 12, sunlight enters the photovoltaic cell through the transparent, rectifying contact 56 and passes to the laser scanned semiconductor film 54 where a photovoltaic current is generated.

Fig. 13 illustrates diagrammatically an alternative procedure for fabricating a photovoltaic cell employing the laser scanning procedures described herein, and Fig. 14 illustrates the cell itself. In this fabrication procedure, a transparent, conductive substrate 60 is used which can be formed by depositing on transparent support 62 a conductive layer 64. Transparent support 62 can be glass or transparent plastic and conductive layer 64 can be a thin layer of a conductive metal. Preferably, a conductive layer 64 is a material which will also form a rectifying contact with a semiconductor layer subsequently deposited thereon. A layer of tin-doped indium oxide, as previously mentioned, would serve as a conductor and would also form a Schottky barrier with some semiconductors such as silicon. Alternatively, another layer which is capable of forming a rectifying contact with the semiconductor could be deposited on to conductive layer 64. Of course, one material which is transparent, conductive and capable of forming a rectifying contact with the semiconductor layer could also be used. Also, the rectifying contact required can

be formed upon deposition of the semiconductor film, or alternatively, in a post treatment of the film. In fact, one suitable post treatment is the laser scanning of the semiconductor film.

A semiconductor film 66, such as a thin film of amorphous silicon, is then deposited on top of transparent, conductive substrate 60. As noted previously, many of the known processes for depositing semi-conductor films can be used since the usual limitations on crystal perfection are obviated with subsequent laser scanning of the film.

The semiconductor film 66 is then scanned with a focused laser beam from a high power laser to improve the film's crystalline properties. Lastly, a conductive layer 68, such as aluminum or other metal, is formed on top of laser-scanned semiconductor film 66. As can be seen in Fig. 14, sunlight enters this photovoltaic cell through the transparent, conductive substrate 60.

Fig. 15 illustrates diagrammatically still another alternative procedure for fabricating a photovoltaic cell employing the laser scanning procedures described herein, and Fig. 16 illustrates the cell produced thereby. In this procedure, an amorphous semiconductor layer 70 is deposited on a substrate 72 which could be a metal or heavily-doped semiconductor. This deposited layer 70 might comprise, for example, a p^- germanium layer having a thickness between 0.1 and 500 μm and being formed from amorphous germanium doped with p-dopants to a carrier level of about 10^{18} carriers/cm^3 or greater. The amorphous germanium layer 70 is then scanned with a high power laser beam as described herein to provide a crystalline semiconductor layer 70. Subsequently, a gallium arsenide layer 74 is applied to the germanium substrate by chemical vapor deposition or other deposition technique. The p layer of gallium arsenide 74 can then be diffused with n-type dopant to form a shallow homojunction therein, or a separate n^+ GaAs layer 76 can be deposited. An ohmic contact 78 is then attached, and an anti-reflection coating 80 can be deposited upon the light receiving surface of the cell.

Although much of the actual experimental work described herein was performed employing amorphous germanium films, similar effects were observed in gallium arsenide and silicon films. It is also believed that other semiconductors could be crystallized by the method of this invention, including, but not limited to, indium phosphide, cadmium sulfide, cadmium telluride, gallium phosphide, germanium/silicon alloy, etc. Moreover, the invention described herein can also be employed in the crystallization of amorphous materials which are not semiconductor materials. These include: inorganic oxides or nitrides such as aluminum oxide or silicon dioxide; amorphous carbon; and even amorphous metals.

It should also be recognized that the invention is suitable with materials which are not 100 percent amorphous, including mixtures of amorphous and crystalline materials. In certain cases, the latent heat liberated upon crystallization might even cause further reaction of materials.

Similarly, although the work described above was performed with laser beams from a Nd:YAG laser, other lasers could be employed, as well as other energy beams. Examples of other suitable energy beams include ion beams, electron beams, or trains of electrical pulses which simulate moving energy beams.

Often, it is desirable to heat the substrate to an elevated temperature, but this must always be below T_c. The energy beam then supplies sufficient energy to heat the amorphous material above T_c. In addition, one possible method is to scan the energy beam at a velocity as fast as the crystallization front velocity v_{ac} in order to maintain the control of the front propagation.

In certain cases, it would be advantageous to modulate the rapidly scanning beam to maintain even better control of the front propagation. In some of these cases; it is preferable to employ a spatially and temporally modulated beam, as is schematically illustrated in Fig. 17. As illustrated in Fig. 17(a), the energy beam initially has a high intensity causing initiation of crystallization and advancement of the crystallization front to a position in front of the beam. At a later time, the beam intensity is lowered but the crystallization front advances further ahead of the beam, as in Fig. 17(b). At a still later time and before the film quenches to cause periodic structure, the beam is advanced and almost catches the crystallization front; as shown in Fig. 17(c). In Fig. 17(d), the laser intensity is increased and the crystallization front again moves away from the beam, in Fig. 17(e), the laser intensity is decreased but before quenching can occur, the beam is moved towards the front, as in Fig. 17(f). Such spatial and temporal modulation is continued, as shown in Fig. 17(g)—Fig. 17(k), until the desired crystallization has been completed. In this manner, the quenching of the film to a temperature below T_c is avoided at one extreme whereas runaway crystallization is avoided at the other extreme.

Fig. 18 illustrates an apparatus suitable for crystallizing amorphous materials by an electron or ion beam. This apparatus is contained within a vacuum chamber 80. Gun 82 can be an electron or ion beam gun, which produces energy beam 84. Beam 84 is focused by focusing means 86 and caused to scan by scanning means 88. Sample 90 is the amorphous material to be crystallized and is supported on sample holder 92 which has resistance heater 94 therein to heat sample 90. In the case where gun 82 is an ion beam gun, simultaneous doping of a semiconductor is possible.

Fig. 19 illustrates still another embodiment of apparatus suitable for carrying out the invention. In this apparatus, a series of voltage sources 100, 100', 100'', 100''' are employed to consecutively apply electrical pulses to conducting pad sets 102, 102', 102'', 102'''. This simulates a moving beam of energy thereby causing a crystallization front to move along amorphous material 104, if the appropriate conditions are chosen.

Industrial applicability

The invention described herein has industrial applicability in the conversion of amorphous materials, such as semiconductor films, to crystalline materials. As described above, such crystalline semiconductor films are employed in photovoltaic devices. It also has industrial applicability in the very rapid conversion of amorphous materials other than semiconductor materials to a crystalline state.

Claims

1. A method of converting solid amorphous material, without melting it, to a more crystalline state, wherein the material is maintained at a first temperature and is irradiated with an energy beam which is scanned over the material to raise it to a second temperature whereat crystal growth occurs within the influence of the beam, characterised by keeping the material at a background temperature T_b below a runaway temperature T_r at which self-sustaining crystallization occurs and by the energy beam having an intensity sufficient to raise the material locally to a critical temperature T_c at which transformation to a crystalline state occurs instantaneously, whereby a crystallization front travels in advance of the beam, the rate at which the beam is scanned being such that before the temperature at the crystallization front quenches below T_c, the material adjacent the advancing crystallization front is heated by the beam sufficiently to prevent the temperature thereat quenching below T_c, the prevention of quenching avoiding the formation of a periodic crystallization structure.

2. A method according to claim 1, wherein the material is a semiconductor film in particular supported on a substrate.

3. A method according to claim 1, wherein the material is selected from carbon, metals, silicon, germanium, a germanium-silicon alloy and gallium arsenide.

4. A method according to claim 1, 2 or 3, wherein the energy beam is a laser beam, electron beam, ion beam, train of electrical pulses, or a combination thereof.

5. A method according to any of claims 1 to 4, wherein the energy beam is shaped to a focussed image on the material, the image having a high aspect ratio in particular greater than 10:1.

6. A method according to any of claims 1 to 5, wherein the energy beam is provided by a continuous wave Nd:YAG laser.

7. A method according to any of claims 1 to 6, wherein the energy beam is scanned over the material by moving the beam relative to the material, by moving the material relative to the beam or by moving both the beam and the material.

8. A method according to any of claims 1 to 7, wherein the material is heated to a temperature T_b by a source of heat other than the energy beam.

9. A method of fabricating a photovoltaic cell, comprising:
(a) either forming a conductive layer on a substrate or selecting a conductive substrate;
(b) forming an amorphous semiconductor film on the conductive layer or conductive substrate;
(c) converting the film to a more crystalline state by the method according to claim 1; and
(d) thereafter forming a transparent rectifying contact on the film.

10. A method of fabricating a photovoltaic cell, comprising:
(a) forming an amorphous semiconductor film on transparent conductive substrate;
(b) forming a rectifying contact between the film and substrate;
(c) converting the film to a more crystalline state by the method according to claim 1; and
(d) forming a conductive layer on the film.

11. A method of fabricating a photovoltaic cell, comprising:
(a) forming an amorphous semiconductor layer;
(b) converting the layer to a more crystalline state by the method according to claim 1, to form a crystalline semiconductor substrate;
(c) forming an active semiconductor film on the substrate;
(d) forming a p-n junction, e.g. a shallow homojunction in the active film; and
(e) forming an ohmic contact on the active film.

Patentansprüche

1. Verfahren zum Umwandeln eines festen amorphen Materials ohne Aufschmelzung in einen kristallineren Zustand, bei dem das Material auf einer ersten Temperatur gehalten und mit einem Energiestrahl bestrahlt wird, mit dem das Material abgetastet wird, um es auf eine zweite Temperatur anzuheben, bei der ein Kristallwachstum innerhalb des Einflusses des Strahls stattfindet, dadurch gekennzeichnet, daß das Material auf einer Grundtemperatur T_b unterhalb einer Durchgehtemperatur T_r gehalten wird, bei der eine selbständige Kristallisation stattfindet, und daß der Energiestrahl eine solche Stärke besitzt, daß das Material örtlich auf eine kritische Temperatur T_c angehoben wird, bei der eine Umwandlung in einen kristallinen Zustand augenblicklich stattfindet, wodurch eine Kristallisationsfront vor dem Strahl herläuft und wobei die Geschwindigkeit, mit der die Strahlabtastung durchgeführt wird, derart bemessen ist, daß, bevor die Temperatur an der Kristallisationsfront unter T_c abfällt, das an die fortschreitende Kristallisationsfront angrenzende Material durch den Strahl derart erwärmt wird, daß

verhindert wird, daß die Temperatur dort unter T_c abfällt, wobei die Verhinderung der Abkühlung die Bildung einer periodischen Kristallisationsstruktur vermeidet.

2. Verfahren nach Anspruch 1, dadurch gekennzeichnet, daß das Material ein Halbleiterfilm insbesondere in Abstützung auf einem Substrat ist.

3. Verfahren nach Anspruch 1, dadurch gekennzeichnet, daß das Material aus Kohlenstoff, Metallen, Silizium, Germanium, einer Germanium-Silizium-Legierung und Galliumarsenid ausgewählt wird.

4. Verfahren nach Anspruch 1, 2 oder 3, dadurch gekennzeichnet, daß als Energiestrahl ein Laserstrahl, ein Elektronenstrahl, ein Ionenstrahl, eine Folge elektrischer Impulse oder eine Kombination hiervon verwendet wird.

5. Verfahren nach einem der Ansprüche 1 bis 4, dadurch gekennzeichnet, daß der Energiestrahl zu einem gebündelten Profil auf dem Material geformt wird und das Profil ein hohes Seitenverhältnis von insbesondere mehr als 10:1 aufweist.

6. Verfahren nach einem der Ansprüche 1 bis 5, dadurch gekennzeichnet, daß der Energiestrahl von einem Dauerstrich-Nd:YAG-Laser bereitgestellt wird.

7. Verfahren nach einem der Ansprüche 1 bis 6, dadurch gekennzeichnet, daß die Abtastung des Materials durch den Energiestrahl dadurch erfolgt, daß der Strahl in bezug auf das Material bewegt wird, das Material in bezug auf den Strahl bewegt wird oder sowohl der Strahl als auch das Material bewegt werden.

8. Verfahren nach einem der Ansprüche 1 bis 7, dadurch gekennzeichnet, daß das Material auf die Temperatur T_b durch eine andere Wärmequelle als der Energiestrahl erwärmt wird.

9. Verfahren zum Herstellen eines Fotoelements, dadurch gekennzeichnet, daß

a) entweder eine leitfähige Schicht auf einem Substrat gebildet oder ein leitfähiges Substrat ausgewählt wird;

b) ein amorpher Halbleiterfilm auf der leitfähigen Schicht oder dem leitfähigen Substrat gebildet wird;

c) der Film durch das Verfahren gemäß Anspruch 1 in einen kristallineren Zustand umgewandelt wird; und

d) danach ein transparenter Gleichrichterkontakt auf dem Film gebildet wird.

10. Verfahren zum Herstellen eines Fotoelements, dadurch gekennzeichnet, daß

a) ein amorpher Halbleiterfilm auf einem transparenten leitfähigen Substrat gebildet wird;

b) ein Gleichrichterkontakt zwischen dem Film und dem Substrat gebildet wird;

c) der Film durch das Verfahren gemäß Anspruch 1 in einen kristallineren Zustand umgewandelt wird; und

d) eine leitfähige Schicht auf dem Film gebildet wird.

11. Verfahren zum Herstellen eines Fotoelements, dadurch gekennzeichnet, daß

a) eine amorphe Halbleiterschicht gebildet wird;

b) die Schicht durch das Verfahren gemäß Anspruch 1 in einen kristallineren Zustand umgewandelt wird, um ein kristallines Halbleitersubstrat zu bilden;

c) ein aktiver Halbleiterfilm auf dem Substrat gebildet wird;

d) ein PN-Übergang, z.B. ein flacher Homoübergang, in dem aktiven Film gebildet wird; und

e) ein Ohm'scher Kontakt auf dem aktiven Film gebildet wird.

Revendications

1. Procédé pour convertir un matériau solide amorphe, sans le fondre, en un état plus cristallin, dans lequel le matériau est maintenu à une première température et est irradié avec un faisceau énergétique au moyen duquel on balaye le matériau, afin de le porter à une seconde température à laquelle apparaît une croissance d'un cristal sous l'influence du faisceau, caractérisé en ce que l'on maintient le matériau à une température de fond T_b inférieure à une température de propagation générale T_r à laquelle apparaît une cristallisation auto-entretenue et en ce que le faisceau énergétique a une intensité suffisante pour porter localement le matériau à une température critique T_c à laquelle le transformation en un état cristallin apparaît instantanément, si bien qu'un front de cristallisation se déplace en avant du faisceau, la vitesse à laquelle le faisceau effectue son balayage, étant telle que, avant que la température à l'emplacement du front de cristallisation ne tombe en dessous de la température critique T_c, le matériau adjacent au front de cristallisation avançant est chauffé suffisamment par le faisceau pour empêcher que la température à cet emplacement ne tombe en dessous de la température critique T_c, l'empêchement de cette chute de température évitant la formation d'une structure de cristallisation périodique.

2. Procédé suivant la revendication 1 caractérisé en ce que le matériau est un film semi-conducteur supporté en particulier sur un substrat.

3. Procédé suivant la revendication 1 caractérisé en ce que le matériau est choisi parmi le carbone, les métaux, le silicium, le germanium, un alliage germanium-silicium et l'arséniure de gallium.

4. Procédé suivant l'une quelconque des revendications 1, 2 ou 3 caractérisé en ce que le faisceau énergétique est un faisceau laser, un faisceau d'électrons, un faisceau d'ions, un train d'impulsions électriques ou une combinaison de ceux-ci.

5. Procédé suivant l'une quelconque des revendications 1 à 4 caractérisé en ce que le faisceau

énergétique est conformé de manière à constituer une image focalisée sur le matériau, cette image ayant un rapport d'aspect élevé en particulier supérieur à 10:1.

6. Procédé suivant l'une quelconque des revendications 1 à 5 caractérisé en ce que le faisceau énergétique est fourni par un laser à onde continue du type Nd:YAG.

7. Procédé suivant l'une quelconque des revendications 1 à 6 caractérisé en ce qu'on effectue le balayage du faisceau énergétique sur le matériau en déplaçant le faisceau par rapport au matériau, en déplaçant le matériau par rapport au faisceau ou en déplaçant à la fois le faisceau et le matériau.

8. Procédé suivant l'une quelconque des revendications 1 à 7 caractérisé en ce que le matériau est chauffé à la température T_b par une source de chaleur autre que le faisceau énergétique.

9. Procédé de fabrication d'une pile photovoltaïque caractérisé en ce qu'il comprend les étapes consistant à:

a) soit former une couche conductrice sur un substrat soit sélectionner un substrat conducteur;
b) former un film semi-conducteur amorphe sur la couche conductrice ou le substrat conducteur;
c) convertir le film en un état plus cristallin par le procédé suivant la revendication 1;
d) former ensuite un contact redresseur transparent sur le film.

10. Procédé de fabrication d'une pile photovoltaïque caractérisé en ce qu'il comprend les étapes consistant à:

a) former un film semi-conducteur amorphe sur un substrat conducteur transparent;
b) former un contact redresseur entre le film et le substrat;
c) convertir le film en un état plus cristallin par le procédé suivant la revendication 1;
d) former une couche conductrice sur le film;

11. Procédé de fabrication d'une pile photovoltaïque caractérisé en ce qu'il comprend les étapes consistant à:

a) former une couche semi-conductrice amorphe;
b) convertir la couche en un état plus cristallin par le procédé suivant la revendication 1, afin de former un substrat semi-conducteur cristallin;
c) former un film semi-conducteur actif sur le substrat;
d) former une jonction p-n, par exemple une homojonction peu profonde, dans le film actif; et
e) former un contact ohmique sur le film actif.

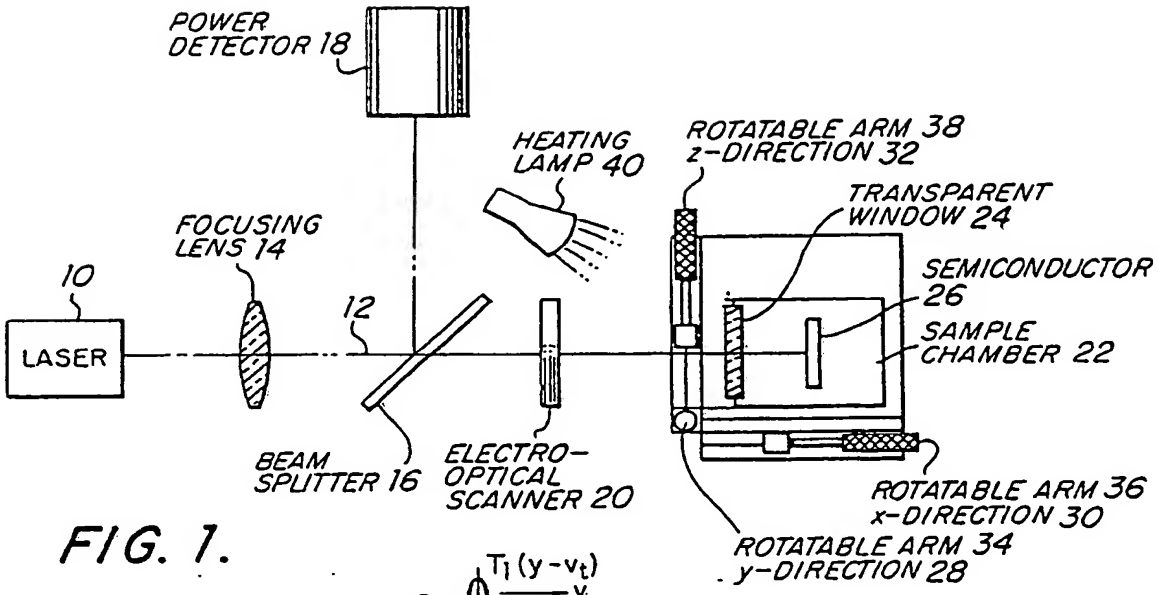

FIG. 1.

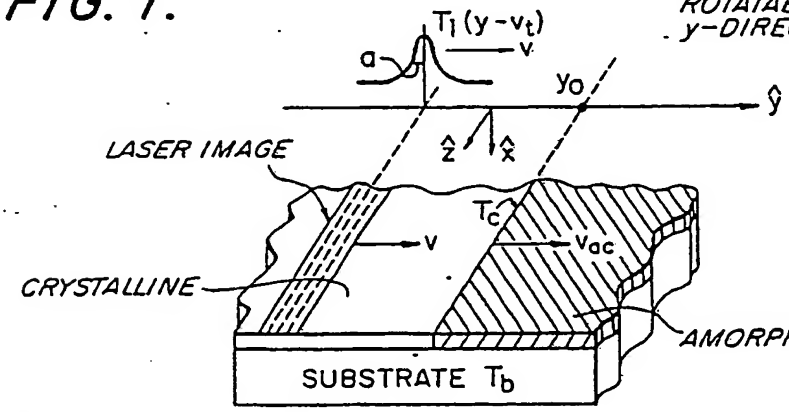

FIG. 7.

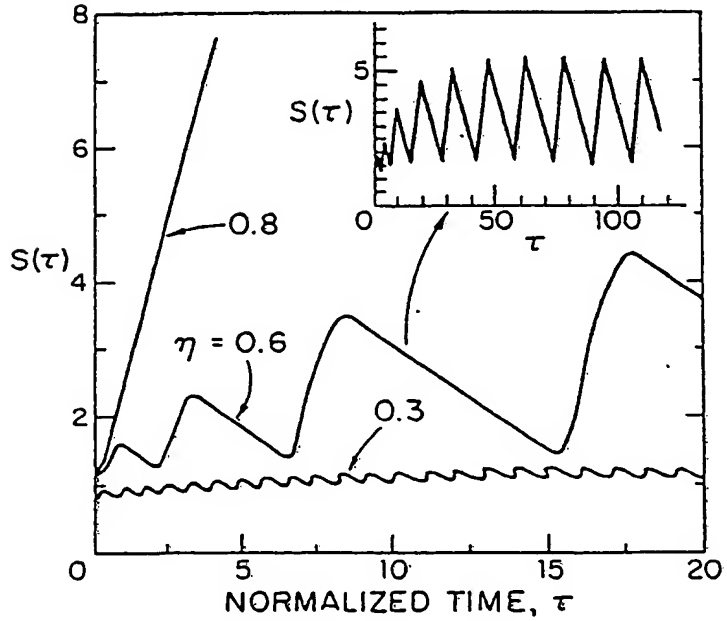

FIG. 8.

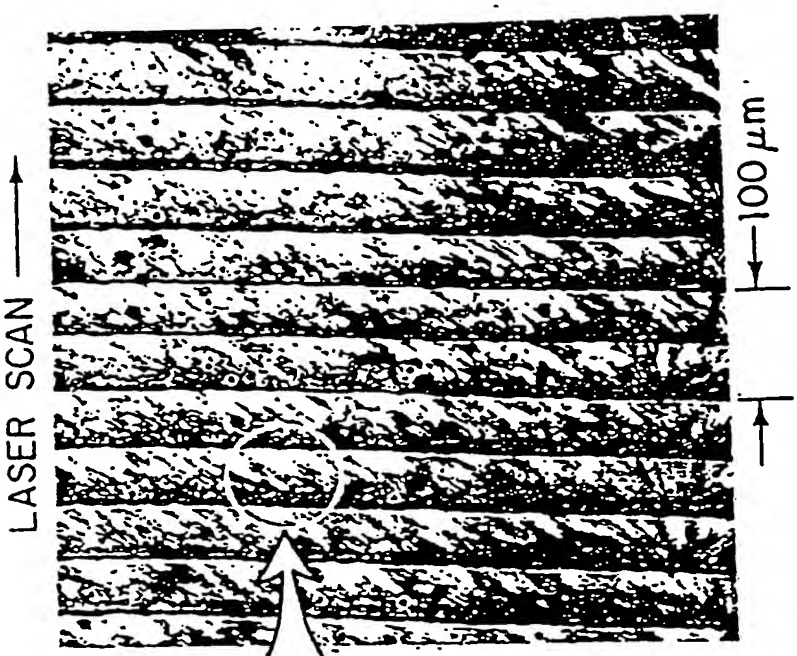
LASER SCAN
100 μm

FIG. 2.

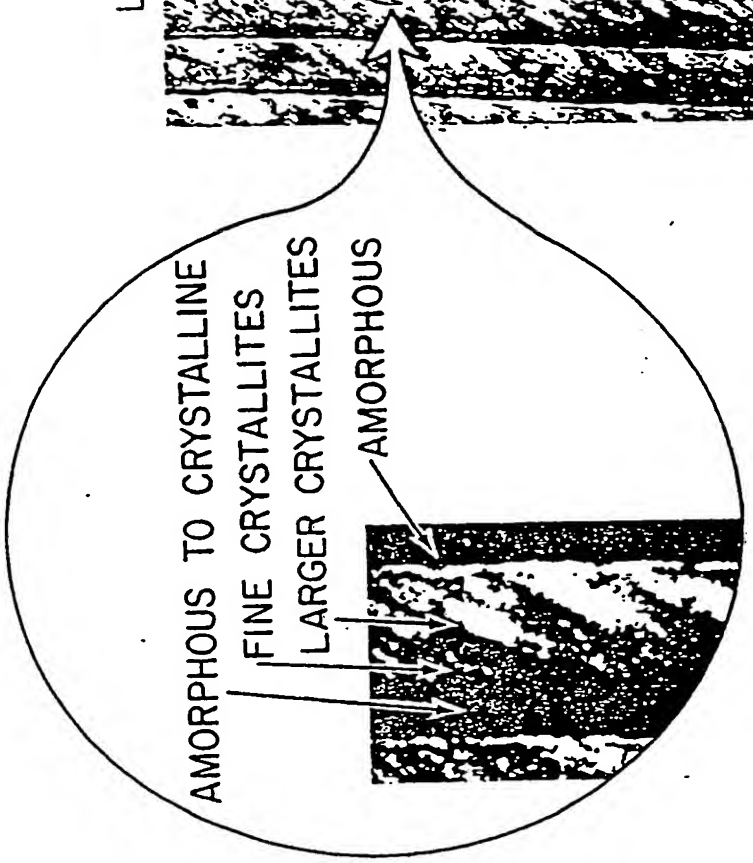
AMORPHOUS TO CRYSTALLINE
FINE CRYSTALLITES
LARGER CRYSTALLITES
AMORPHOUS

FIG. 3.

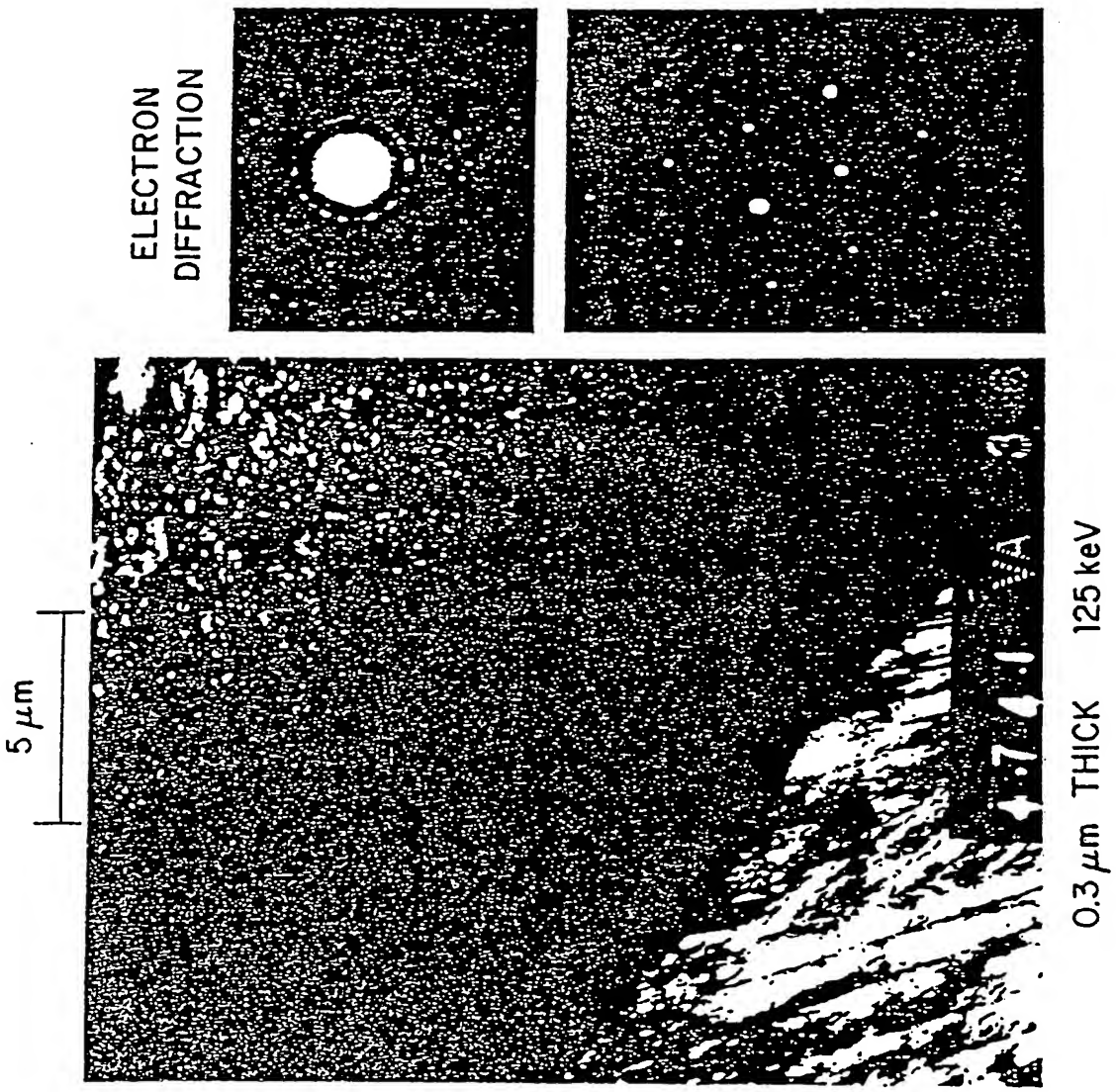

FIG. 5.

FIG. 6.

FIG. 4.

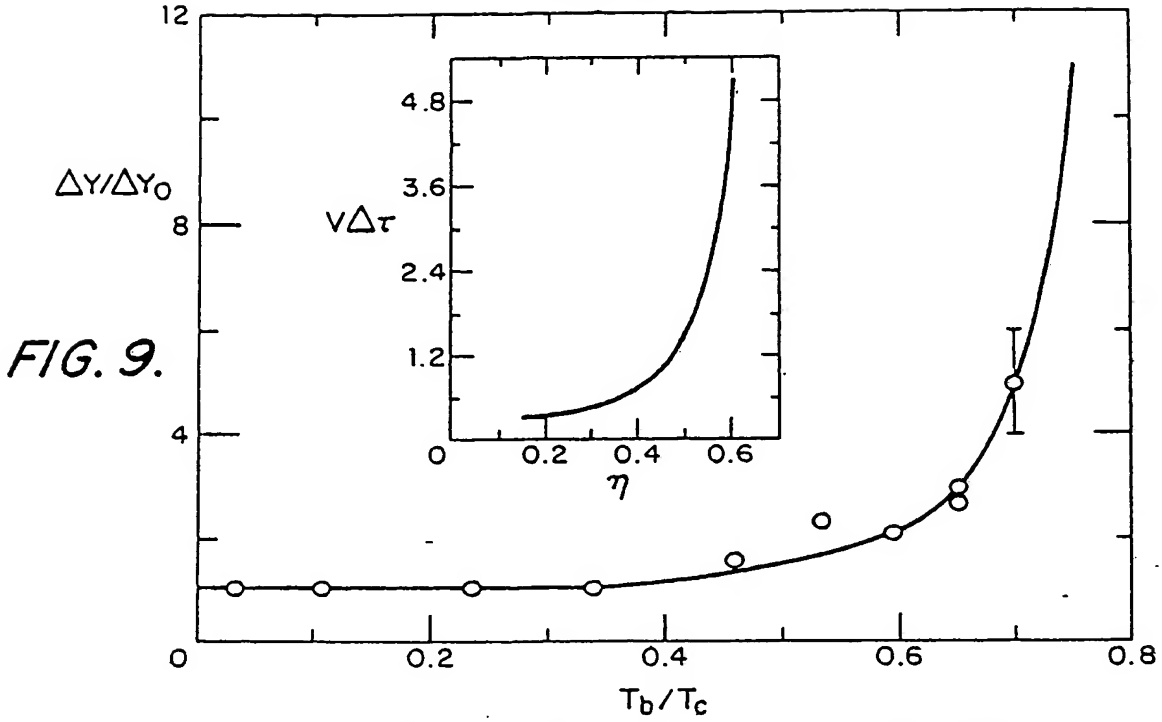

FIG. 9.

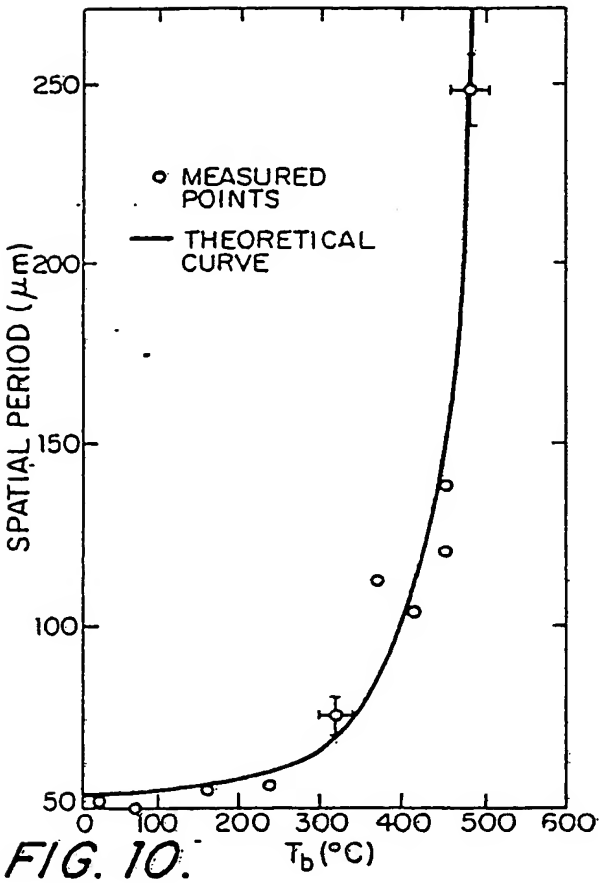

FIG. 10.

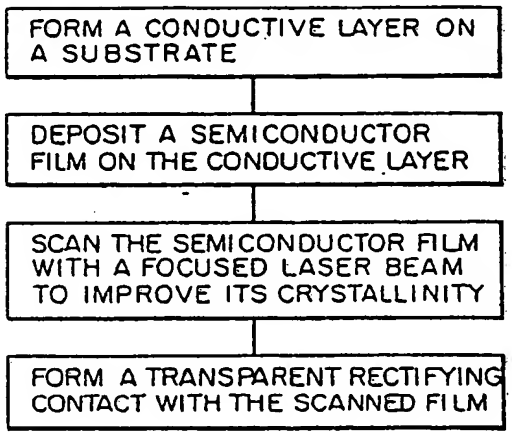

FIG. 11.

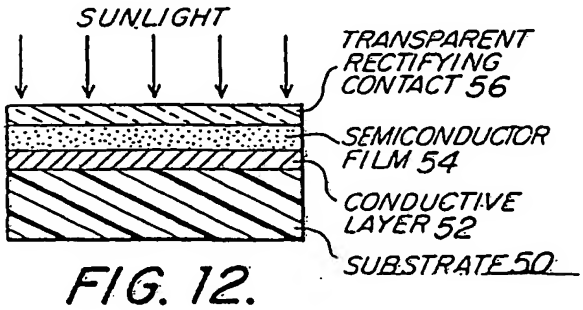

FIG. 12.

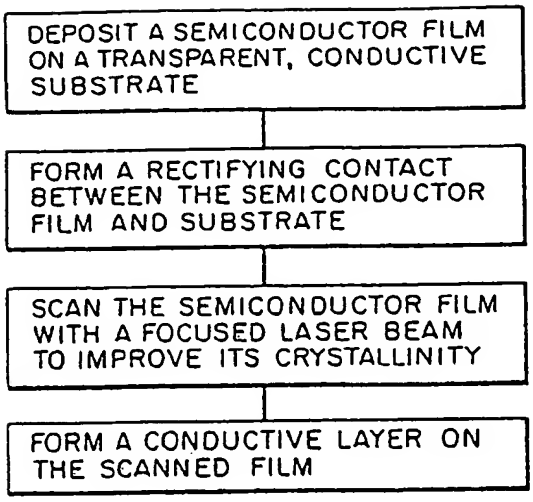

FIG. 13.

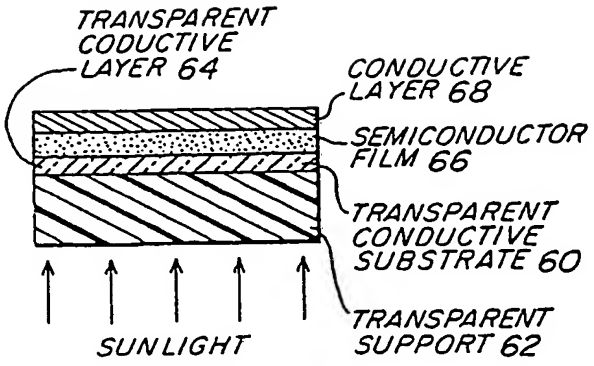

FIG. 14.

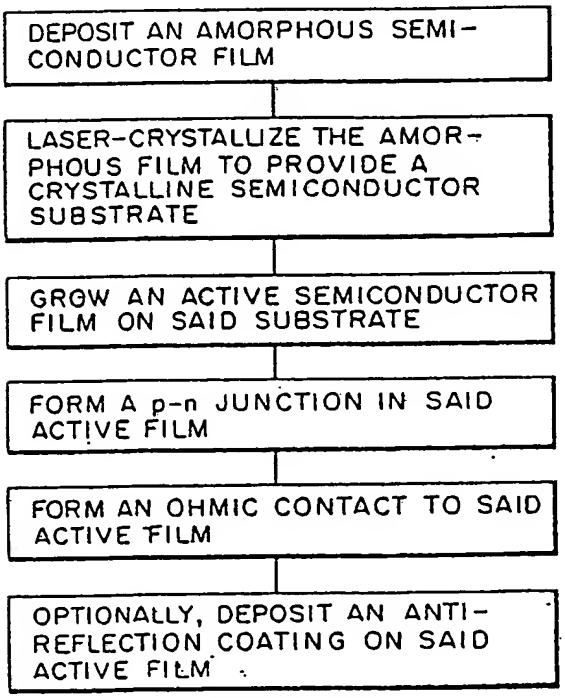

FIG. 15.

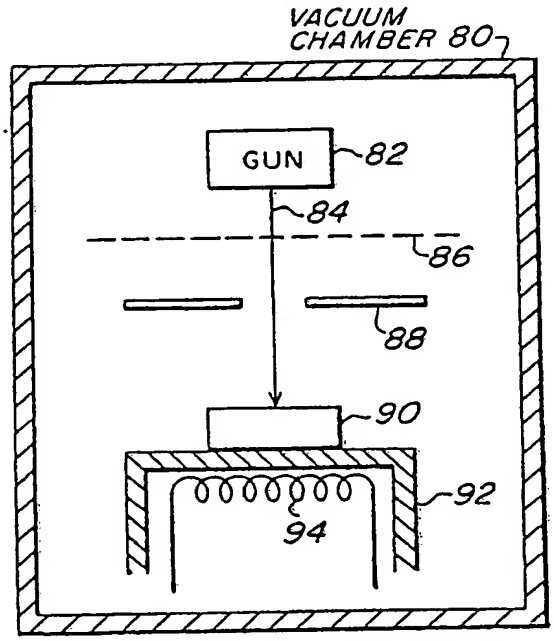

FIG. 18.

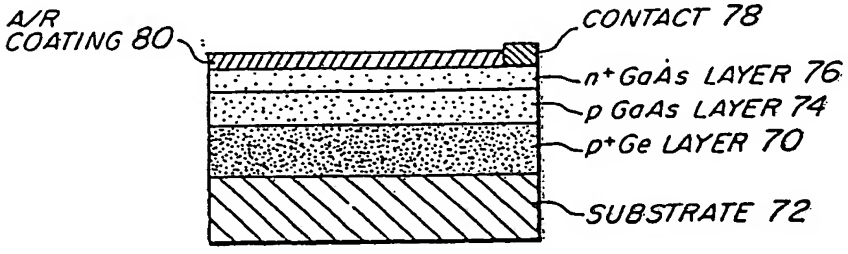

FIG. 16

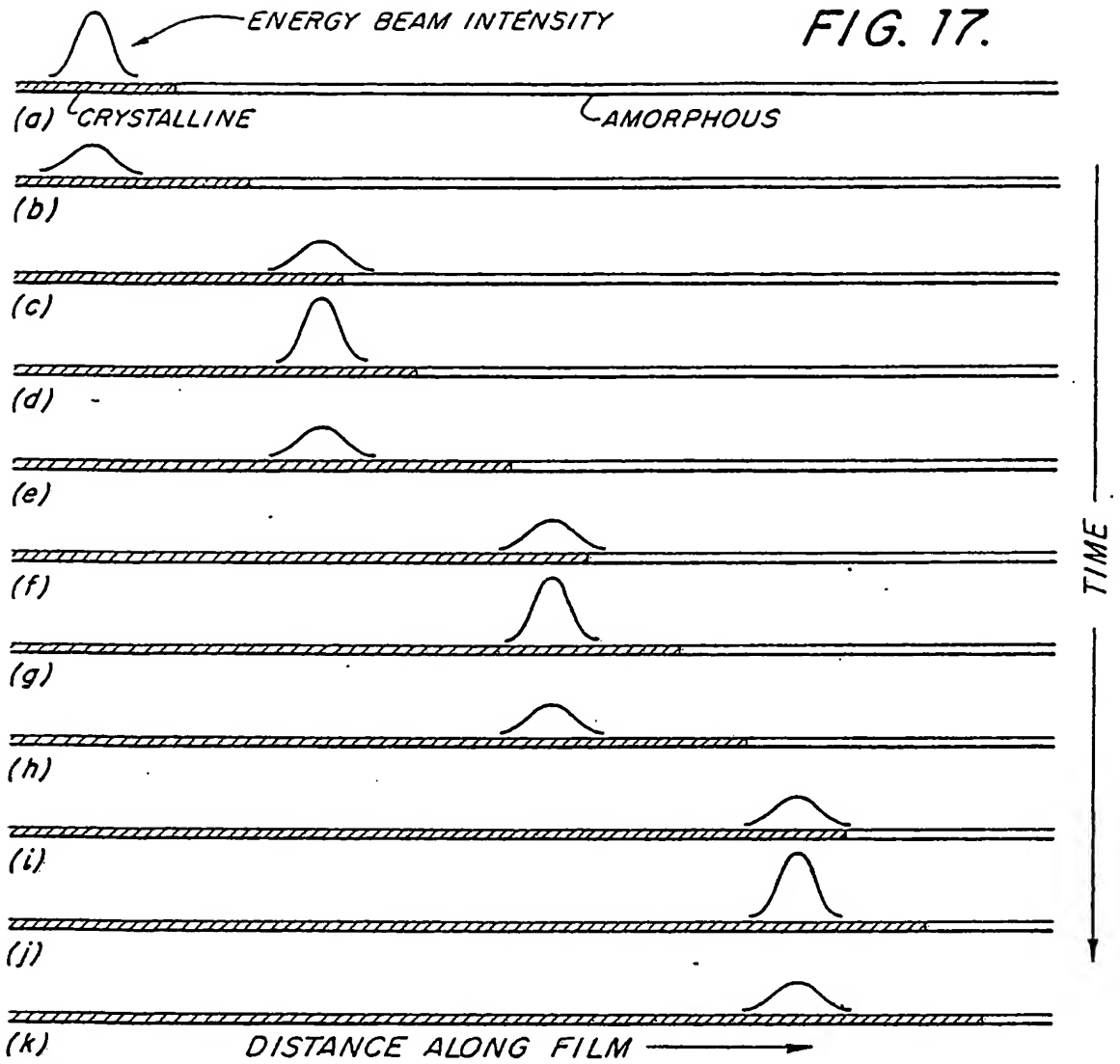
ENERGY BEAM INTENSITY
(a)
CRYSTALLINE
AMORPHOUS
(b)
(c)
(d)
(e)
(f)
(g)
(h)
(i)
(j)
(k)
TIME
DISTANCE ALONG FILM

FIG. 17.

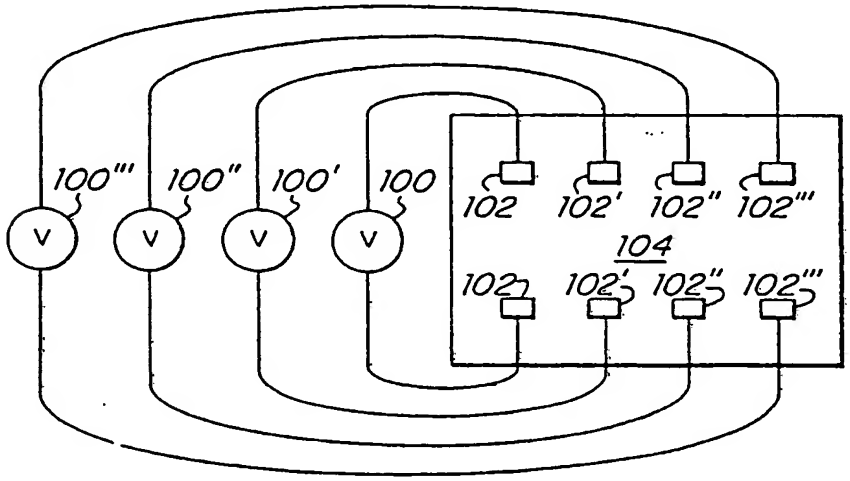
100'''
100''
100'
100
V
V
V
V
102
102'
102''
102'''
104
102
102'
102''
102'''

FIG. 19.